

# ANALYSIS AND EXPERIMENTAL TESTING OF INSULATED PRESSURE VESSELS FOR AUTOMOTIVE HYDROGEN STORAGE

S. M. Aceves  
Lawrence Livermore National Laboratory  
7000 East Ave., L-641  
Livermore, CA 94551, USA  
[saceves@llnl.gov](mailto:saceves@llnl.gov)

J. Martinez-Frias  
Centro de Ingenieria y Desarrollo Industria  
Pie de La Cuesta #701  
Queretaro, Queretaro, Mexico  
[jmartinez@cidesi.mx](mailto:jmartinez@cidesi.mx)

O. Garcia-Villazana  
FIMEE, University of Guanajuato  
Department of Mechanical Engineering  
Apartado Postal 215-A  
Salamanca, Guanajuato, Mexico  
[villa@salamanca.ugto.mx](mailto:villa@salamanca.ugto.mx)

## Abstract

This paper presents an analytical and experimental evaluation of the applicability of insulated pressure vessels for hydrogen-fueled light-duty vehicles. Insulated pressure vessels are cryogenic-capable pressure vessels that can be fueled with liquid hydrogen (LH<sub>2</sub>) or ambient-temperature compressed hydrogen (CH<sub>2</sub>). Insulated pressure vessels offer the advantages of liquid hydrogen tanks (low weight and volume), with reduced disadvantages (lower energy requirement for hydrogen liquefaction and reduced evaporative losses).

The purpose of this work is to verify that commercially available aluminum-lined, fiber-wrapped vessels can be used for cryogenic hydrogen storage. The paper reports on previous and ongoing tests and analyses that have the purpose of improving the system design and assure its safety.

The analytical and experimental results carried out until now indicate that it may be possible to use fiber-wrapped aluminum-lined vessels for operation at LH<sub>2</sub> temperature and high pressure. Required future tests are described that will assure vessel safety under daily operating conditions.

## Introduction

Hydrogen-fueled vehicles present features that make them serious candidates as alternatives to today's petroleum-powered vehicles. Hydrogen vehicles can use the advanced technology of electric vehicles to improve environmental quality and energy security, while providing the range, performance, and utility of today's gasoline vehicles.

Probably the most significant hurdle for hydrogen vehicles is storing sufficient hydrogen on board. Hydrogen storage choices can determine the refueling time, cost, and infrastructure requirements, as well as indirectly influence energy efficiency, vehicle fuel economy, performance, and utility. There are at least three viable technologies for storing hydrogen fuel on cars. These are: compressed hydrogen gas ( $\text{CH}_2$ ), metal hydride adsorption, and cryogenic liquid hydrogen ( $\text{LH}_2$ ), but each has significant disadvantages.

Storage of 5 kg of hydrogen (equivalent to 19 liters; 5 gallons of gasoline) is considered necessary for a general-purpose vehicle, since it provides a 320 km (200 mile) range in a 17 km/liter (40 mpg) conventional car; or a 640 km (400 mile) range in a 34 km/liter (80 mpg) hybrid vehicle or fuel cell vehicle. Storing this hydrogen as  $\text{CH}_2$  requires a volume so big that it is difficult to package in light-duty vehicles (Pentastar Electronics, 1997), and heavy-duty trucks. The external volume for a pressure vessel storing 5 kg of hydrogen at 24.8 MPa (3600 psi) is 320 liters (85 gal). Hydrides are heavy (300 kg for 5 kg of hydrogen, Michel et al., 1996), resulting in a substantial reduction in vehicle fuel economy and performance.

Low-pressure  $\text{LH}_2$  storage is light and compact, and has received significant attention due to its advantages for packaging (Braess and Strobl, 1996). Significant recent developments have resulted in improved safety (Pehr, 1996a, 1996b) and fueling infrastructure (Hettinger et al, 1996). Disadvantages of low-pressure  $\text{LH}_2$  storage are: the substantial amount of electricity required for liquefying the hydrogen (Peschka, 1992); the evaporation losses that may occur during fueling low-pressure  $\text{LH}_2$  tanks (Wetzel, 1996); and the evaporation losses that occur during long periods of inactivity, due to heat transfer from the environment.

An alternative is to store hydrogen in an insulated pressure vessel that has the capacity to operate at  $\text{LH}_2$  temperature (20 K), and at high pressure (24.8 MPa; 3600 psi). This vessel has the flexibility of accepting  $\text{LH}_2$  or  $\text{CH}_2$  as a fuel. Filling the vessel with ambient-temperature  $\text{CH}_2$  reduces the amount of hydrogen stored (and therefore the vehicle range) to about a third of its value with  $\text{LH}_2$ .

The fueling flexibility of the insulated pressure vessels results in significant advantages. Insulated pressure vessels have similar or better packaging characteristics than liquid hydrogen tanks (low weight and volume), with reduced energy consumption for liquefaction. Energy requirements for hydrogen liquefaction are lower than for liquid hydrogen tanks because a car with an insulated pressure vessel can use, but does not require, cryogenic hydrogen fuel. A hybrid or fuel cell vehicle (34 km/l, 80 mpg) could be refueled with ambient-temperature  $\text{CH}_2$  at

24.8 MPa (3600 psi) and still achieve a 200 km range, suitable for the majority of trips. The additional energy, costs, and technological effort for cryogenic refueling need only be undertaken (and paid for) when the additional range is required for longer trips. With an insulated pressure vessel, vehicles can refuel most of the time with ambient-temperature hydrogen, using less energy, and most likely at lower ultimate cost than LH<sub>2</sub>, but with the capability of having 3 times the range of room-temperature storage systems.

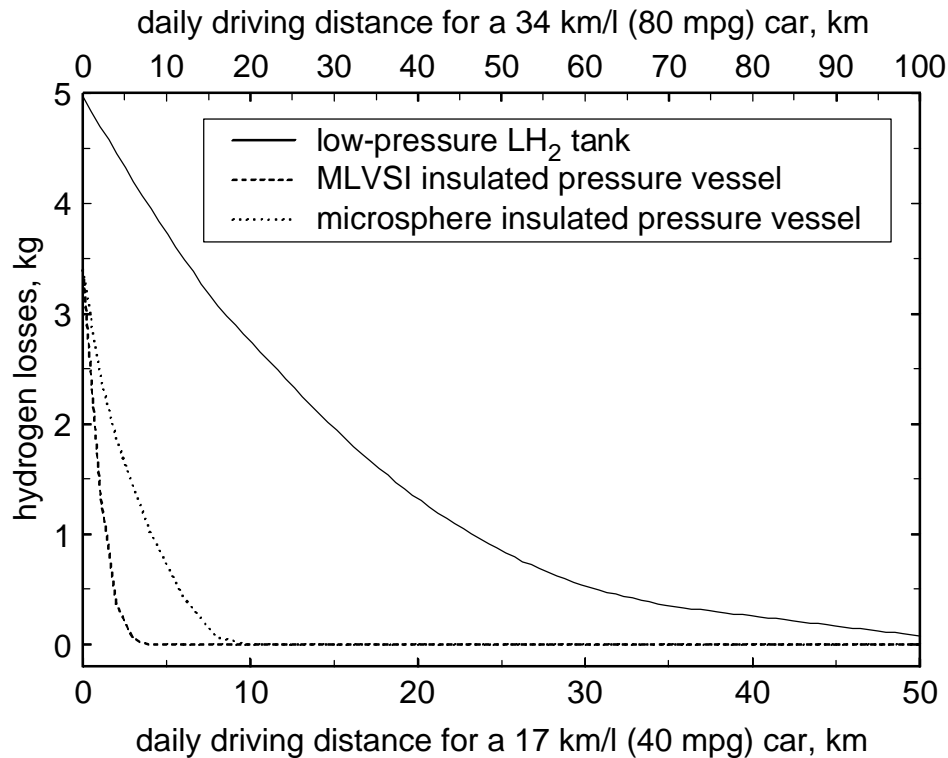


**Figure 1. Cumulative hydrogen losses in kg as a function of daily driving distance, for vehicles with 17 km/liter (40 mpg); or 34 km/l (80 mpg) fuel economy, for three cryogenic hydrogen storage vessels.**

Insulated pressure vessels also have much reduced evaporative losses compared to LH<sub>2</sub> tanks. This has been demonstrated in a previous work (Aceves and Berry, 1998), which presented a thorough analysis of evaporative losses in cryogenic pressure vessels based on the first law of thermodynamics. Figure 1 illustrates some of the main results. This figure shows hydrogen losses during vehicle operation. The figure assumes that three vehicles are fitted with cryogenic hydrogen storage tanks with the same capacity (5 kg). One vehicle has a low-pressure (0.5 MPa; 70 psia) liquid hydrogen tank. The other two vehicles have insulated pressure vessels, one with multilayer vacuum superinsulation (MLVSI), and the other with microsphere insulation. The vehicles are identical in every aspect, except for the tanks. The vessels are filled to full capacity (5 kg) with liquid hydrogen, and then the vehicles are driven a fixed distance every day. When

the fuel runs out, the amount of fuel burned by the engine and the amount of fuel lost to evaporation are calculated, and the results are shown in Figure 1. The figure shows total cumulative evaporative hydrogen losses out of a full tank as a function of the daily driving distance. The figure includes information for 17 km/l and 34 km/l cars respectively in the lower and upper x-axes. As expected, evaporative losses increase as the daily driving distance is reduced, because less driving results in a longer time for hydrogen evaporation. The figure shows that a low-pressure LH<sub>2</sub> tank loses hydrogen even when driven 50 km per day in a 17 km/l car (100 km in a 34 km/l car). Losses from a low-pressure LH<sub>2</sub> tank grow rapidly as the daily driving distance drops. Insulated pressure vessels lose hydrogen only for very short daily driving distances. Even a microsphere-insulated vessel does not lose any hydrogen when driven 10 km/day or more (20 km/day in the 34 km/l car). Since most people drive considerably more than this distance, no losses are expected from insulated pressure vessels under normal operating conditions (Aceves and Berry, 1998).

From an engineering and economic perspective, insulated pressure vessels strike a versatile balance between the cost and bulk of ambient-temperature CH<sub>2</sub> storage, and the energy efficiency, thermal insulation and evaporative losses of LH<sub>2</sub> storage.

Considering all the potential benefits of insulated pressure vessels, it is important to determine what type of pressure vessel can be operated at both high pressure and cryogenic temperature. Of the available pressure vessel technologies commonly used for vehicular storage of natural gas (Institute of Gas Technology, 1996), it appears that aluminum-lined, composite-wrapped vessels have the most desirable combination of properties for this application (low weight and affordable price). However, commercially available aluminum-composite pressure vessels are not designed for low temperature applications.

This paper describes a series of tests that have been done or are being planned for testing whether commercially-available aluminum-fiber pressure vessels can be used at cryogenic temperatures and high pressures, as would be required for vehicular hydrogen storage. The final goal is to demonstrate the benefits of insulated pressure vessels while at the same time guaranteeing safety for the users.

## **Previous and ongoing tests**

### **Pressure and Temperature Cycling**

Pressure vessels have been cycled through 900 high-pressure cycles and 100 low-temperature cycles. The cycles are alternated, running 9 pressure cycles followed by a temperature cycle, and repeating this sequence 100 times. This test is expected to replicate what would happen if these vessels were used in a hydrogen-fueled car. Liquid nitrogen is used for low-temperature cycling and gaseous helium for high-pressure cycling. To accomplish the required testing, an experimental setup has been built inside a high-pressure cell. A schematic is shown in Figure 2. The valves shown in the schematic are controlled by computer, which allows the system to run with no supervision, resulting in fast cycling. An aramid-aluminum and a carbon fiber-aluminum pressure vessel have been cycled. The characteristics of these are listed in Table 1.

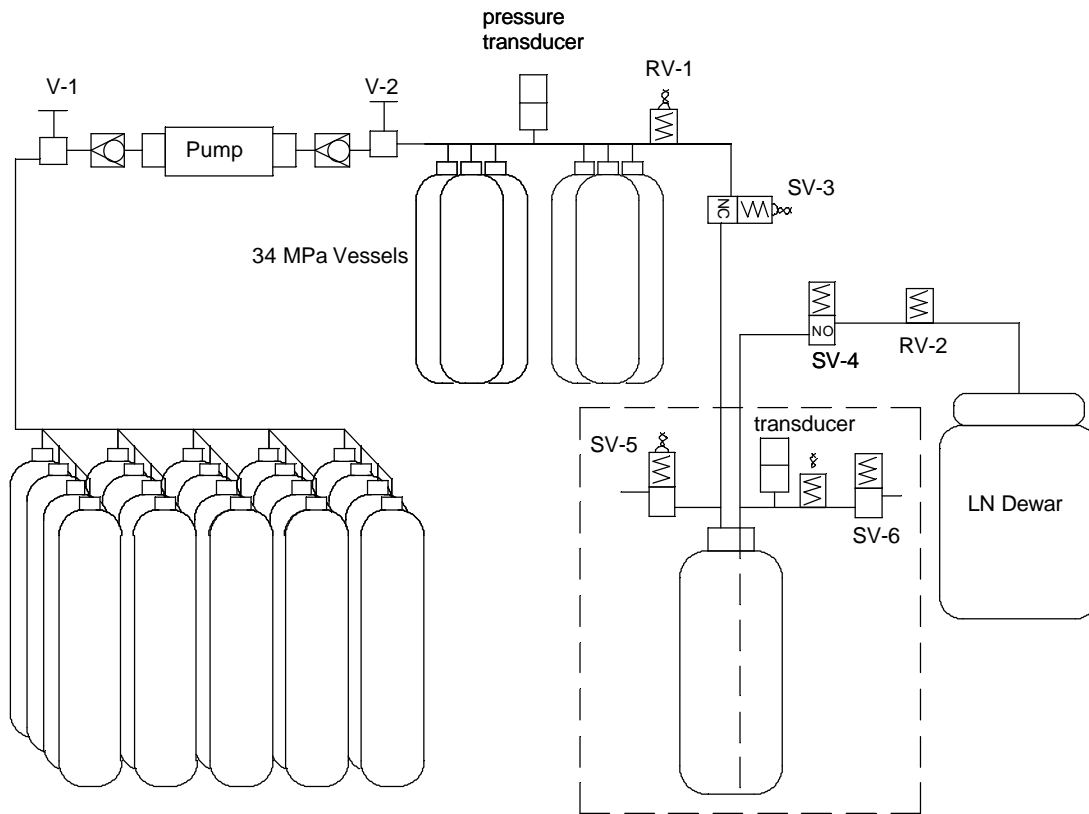


**Figure 2. Schematic of the experimental setup for temperature and pressure cycling of pressure vessels.**

**Table I. Characteristics of the Tested Hydrogen Vessels and their Planned Insulation**

	Aramid- Aluminum	Carbon Fiber- Aluminum
Mass of hydrogen stored, kg	1.13	0.44
Vessel weight, kg	10	4.1
Internal volume, liters	17.6	6.8
Internal diameter, m	0.2	0.17
Internal surface area, m <sup>2</sup>	0.48	0.25
Design pressure, MPa (psi)	24.1 (3500)	31 (4500)
Performance factor <sup>1</sup> , m (10 <sup>6</sup> in)	13000 (0.5)	13115 (0.51)
Safety factor	3.0	2.5
Insulating material	MLVSI <sup>2</sup>	MLVSI <sup>2</sup>
Thermal conductivity of insulator, W/mK	0.0001	0.0001
Insulation thickness, m	0.02	0.02
Heat transfer through accessories, W	0.5	0.5

<sup>1</sup> defined as burst pressure\*volume/weight.

<sup>2</sup> MLVSI = multilayer vacuum superinsulation

Figures 3 and 4 show respectively the variation of pressure and temperature as a function of time for the cyclic test of an aramid-aluminum pressure vessel. The figures show pressure and temperature for 9 consecutive pressure cycles and a cryogenic cycle. This sequence is repeated 100 times for each vessel test. During the pressure cycles, the pressure is increased rapidly to the working pressure and reduced down to a low value. The pressure cycles take about 15 minutes. After the pressure cycles, the vessel is cooled down with liquid nitrogen at ambient pressure. At the end of the cryogenic cycle, the pressure is raised slightly to vent the liquid nitrogen contained in the vessel.

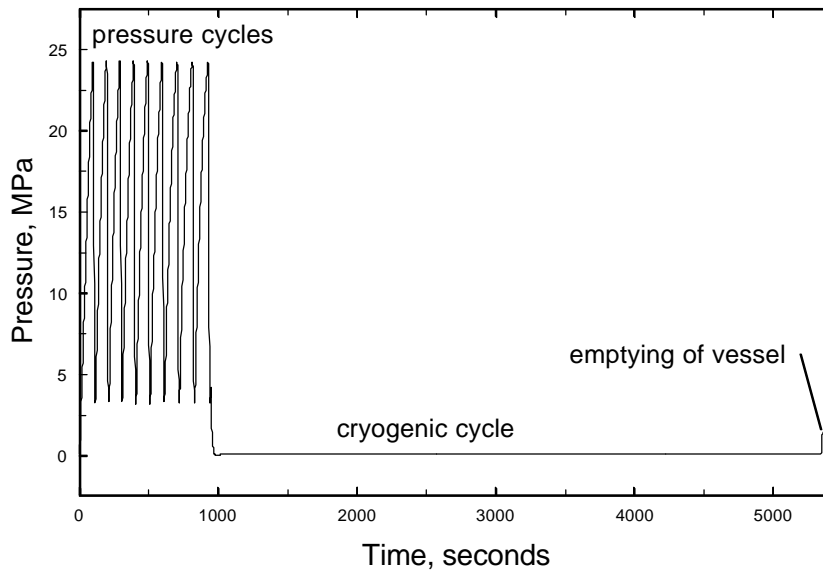


**Figure 3. Pressure as a function of time during cycle testing of the aramid-aluminum pressure vessel.**

Figure 4 shows temperature during the vessel cycling experiment. Temperature was measured with thermocouples in three locations: on the external surface of the pressure vessel (on the fiber-epoxy surface) near the top and near the bottom of the vessel; and on the external surface of the liquid nitrogen (LN<sub>2</sub>) line. For the cyclic test, the vessel was insulated with 2 cm of rubber insulation. Due to the low performance of the rubber insulation, the temperature outside the vessel was significantly higher than the temperature inside the vessel. A preliminary test was performed to verify how cold the external surface of the vessel had to be for the vessel to be full of LN<sub>2</sub>. It was found that cooling the vessel until the external thermocouple indicates  $-80^{\circ}\text{C}$  is necessary for obtaining complete filling of the vessel. This temperature was then used to decide

when the cryogenic cycle was complete. The figure also shows that the temperature of the pressure vessel increases substantially during the pressure cycles due to compression work. This guarantees that all the thermal cycles are initiated at ambient temperature or higher.

Two cyclic tests have been completed to date. The vessels have not failed during the test, and they have not shown superficial evidence of damage under observation. The carbon fiber-aluminum vessel was instrumented with strain gages in addition to the thermocouples and pressure sensor. Results from the strain gages will be used for validating the finite element analysis.

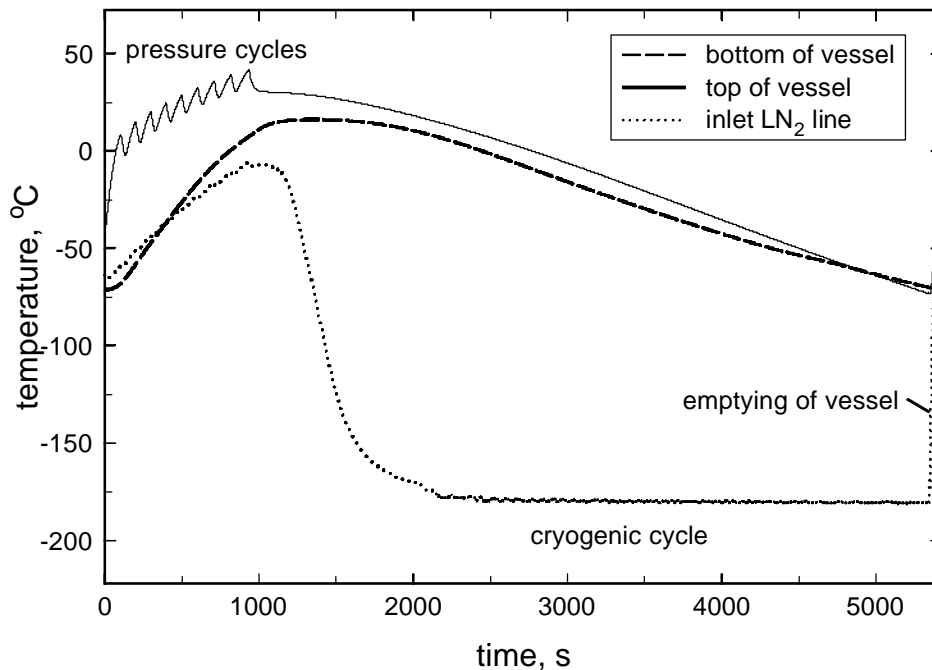


**Figure 4. Temperature as a function of time during cycle testing of the aramid-aluminum pressure vessel. The figure shows three temperatures measured at locations on the external surface of the vessel and inlet liquid nitrogen line.**

## Ultrasound

Cycled vessels have been sent to ultrasound evaluation for a more complete analysis of damage due to cycling. Ultrasonic nondestructive test methods employ high-frequency mechanical vibrational energy to detect and locate structural discontinuities or differences of a variety of materials. An electric pulse is generated in a test instrument and transmitted to a transducer, which converts the electric pulse into mechanical vibration. These low energy-level vibrations are transmitted through a coupling liquid into the test object, where the ultrasonic energy is attenuated, scattered, reflected, or resonated to indicate conditions within the material. Reflected,

transmitted, or resonant sound energy is reconverted to electrical energy by a transducer and returned to the test instrument, where it is amplified. The presence, position, and amplitude of the echoes indicate conditions of the test-object material (Bray and Stanley, 1997).

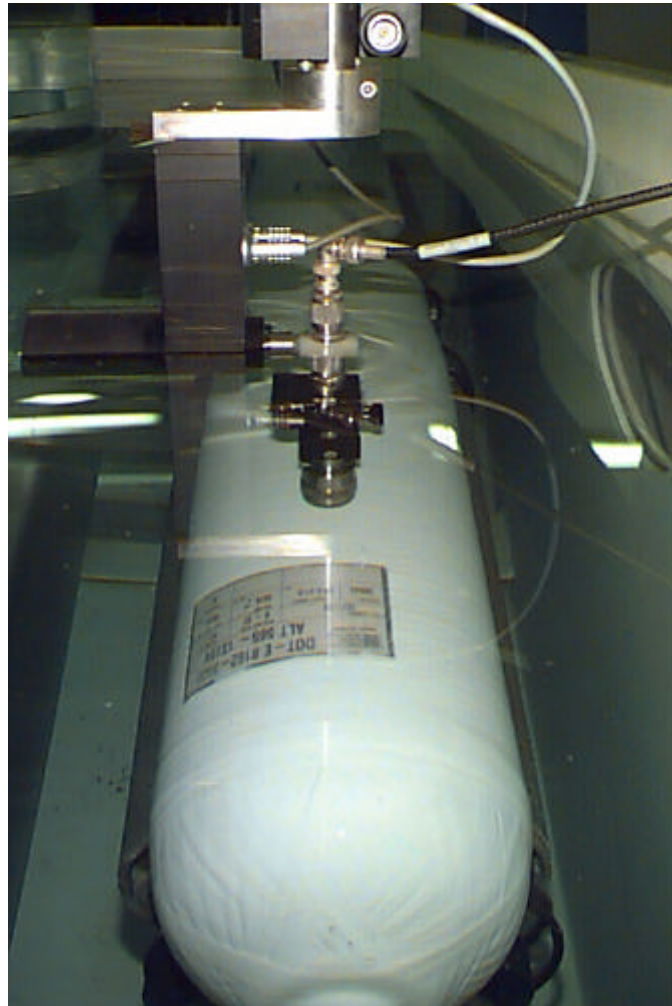


**Figure 5. End view of an aramid filament-wound composite vessel with an aluminum liner being scanned under water in an ultrasonic scanner.**

Two aramid-aluminum vessels were imaged with immersion ultrasonics (Figure 5). One of the vessels had been cycled at high pressure and low temperature, as previously described. The other vessel was used as a control vessel and was not cycled. The vessels were scanned with pulsed echo ultrasound. Ultrasonic data were collected on the cylindrical portion of each vessel using a 1 MHz, 1-inch diameter probe. Figure 6 shows how the transducer was positioned on the cylinder, the direction the data were acquired, and the scan area.



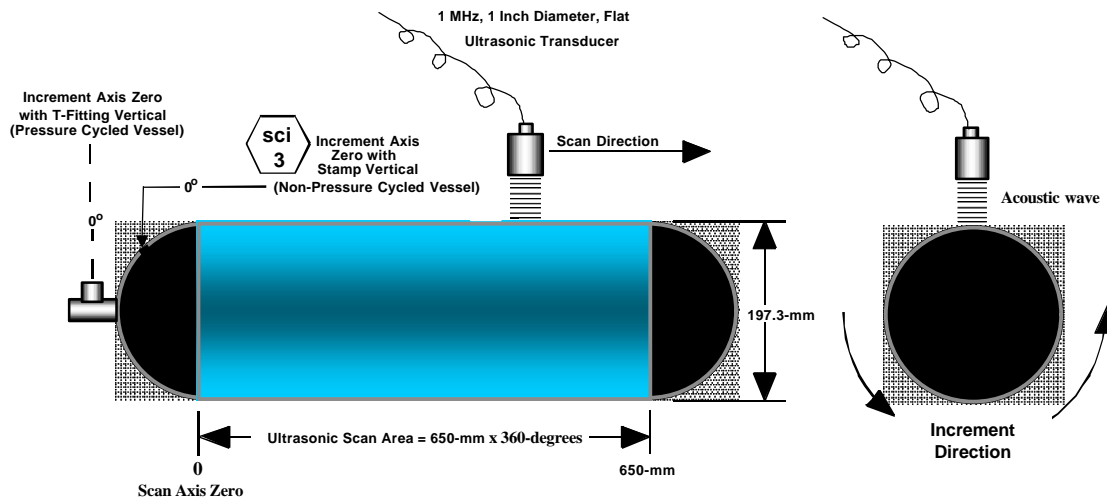


**Figure 6. Schematic of the setup and alignment of an aramid filament wound composite vessel with an aluminum liner during ultrasound testing.**

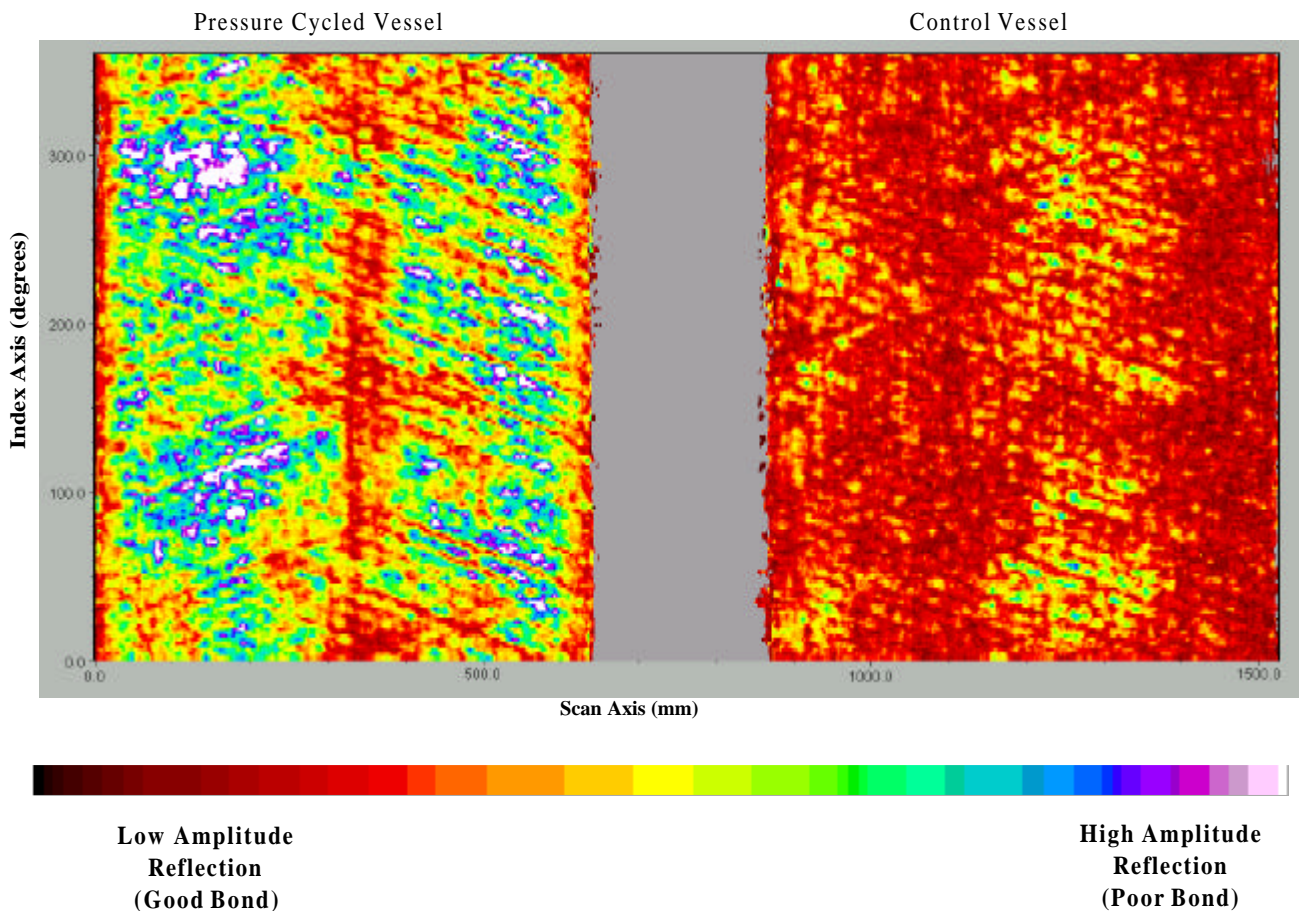


**Figure 7. Ultrasound image of two test vessels: a vessel that was cycled over 1000 pressure and cryogenic cycles, and a pressure vessel that has not been cycled, used for control.**

The ultrasound equipment produces a view of the part that indicates the axial and transversal position of flaws. Flaw depth may be indicated with different shades of gray or different colors. The immersion technique typically uses water as the coupling medium and the probe can be readily indexed for direct input into a data analysis system.

The data displayed in the horizontal (longitudinal) direction of each image were acquired every 1 mm for a total length of 650 mm. The data displayed in the vertical (transversal) direction was acquired every 2 degrees for 360 degrees. Ultrasonic C-scan images of the two vessels are shown in Figure 7. Reflected amplitudes in Figure 7 are mapped according to the gray scale bar. The highest amplitude reflections, indicating delamination within the aramid composite, are shown in white. The lowest amplitude reflection indicating areas of good bond is shown in black. The cycled vessel shows several areas of delamination. The control vessel shows good bond overall with a few locations of partial bond. The figure indicates that cryogenic cycling of the vessel may produce enough stresses within the fiber to result in delamination. However, it is considered that this damage should not cause any reduction in pressure vessel performance at high pressure, because the fibers tend to reattach when the vessel is pressurized. To verify this hypothesis, it is necessary to burst-test the pressure vessels.

### **Burst Test**

The aramid-aluminum and the carbon fiber-aluminum pressure vessels were burst-tested after being cycled and ultrasound-tested. The burst test was conducted according to the Code of Federal Regulations-Department of Transportation standards for pressure vessel certification (CFR-DOT, 1996a). Figure 8 shows the variation of pressure as a function of time for the aramid-aluminum vessel. The burst pressure was 94.17 MPa (13.7 ksi), which is substantially higher than the minimum burst pressure of 72.4 MPa (10.5 ksi). The very high value of the burst pressure compared to the minimum burst pressure may be due in part to work hardening that took place during the cycling of the vessel. The carbon fiber-aluminum also failed at a pressure higher than the minimum required.

### **Finite Element Analysis**

Cyclic, ultrasound and burst testing of the pressure vessels is being complemented with a finite element analysis, which will help to determine the causes of any potential damage to the vessel during low temperature operation. Finite element analysis is currently in progress. A mesh has been built and preliminary runs have been made. Physical properties of fiber-epoxy laminae were obtained from available literature at ambient and cryogenic temperatures (Reed and Golda, 1994, Morgan and Allred, 1989). Lamina properties are then converted into properties of the composite matrix. This is done by using a computer program (Hull and Clyne, 1996). This program assumes that the matrix is a homogeneous, orthotropic material. The properties of the matrix will be used in the finite element thermal and stress analysis. Results of the finite element analysis will be validated by comparison with the strain gage measurements.

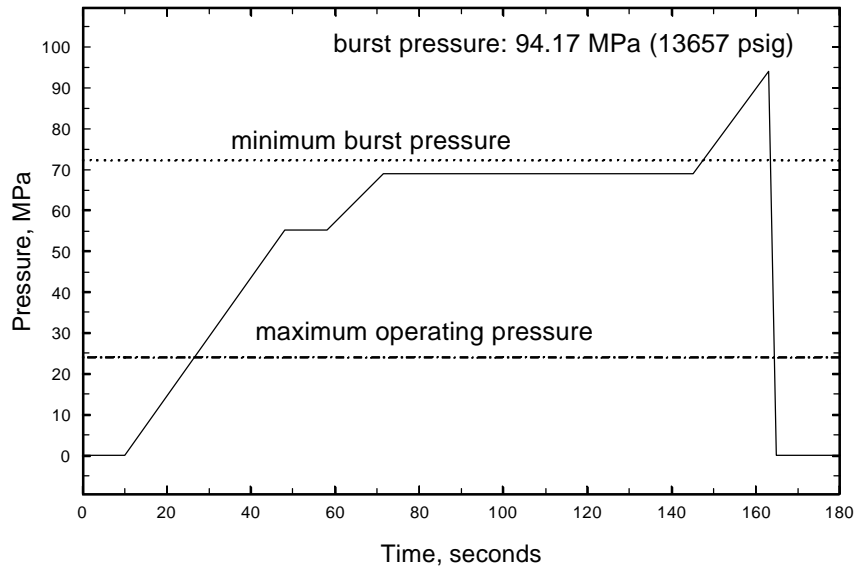


**Figure 8. Pressure as a function of time during the burst test of the aluminum-lined, aramid-wrapped vessel. The burst pressure was 94.17 MPa (13657 psig).**

## Insulation Design

The pressure vessels will be insulated with multilayer vacuum superinsulation (MLVSI). MLVSI has a good thermal performance only under a high vacuum, at a pressure lower than 0.01 Pa ( $7.5 \times 10^{-5}$  mm Hg, Kaganer, 1969). Therefore, the use of MLVSI requires that an outer jacket be built around the vessel. The design of the insulation is shown in Figure 9. The insulation design includes access for instrumentation for pressure, temperature and level, as well as safety devices to avoid a catastrophic failure in case the hydrogen leaks into the vacuum space.

Keeping a vacuum inside the insulation space requires a control of the outgassing of the materials that are in contact with the vacuum. Usually this is a straightforward procedure for vacuum systems that have all surfaces made of metal. However, in this case, one of the surfaces in contact with the vacuum is a fiber-epoxy surface, that is capable of substantial outgassing. In addition to this, the outgassing obtained from this surface is not documented in the literature. To evaluate surface outgassing, a pressure vessel was tested as shown in Figure 10. The test vessel was placed inside a vacuum chamber. A turbo pump was connected to the vacuum chamber, and a calibrated valve was placed between the vacuum chamber and the turbo pump. Vessel outgassing is then determined by measuring the difference in pressure across the calibrated

valve. The results of the outgassing experiment are shown in Figure 11. This figure shows pressure in the vacuum chamber (vessel) and in the turbo pump as a function of time. The figure also shows outgassing rate. The experiment was conducted for 90 hours. The pressure in the vacuum chamber changed little during the length of the experiment, indicating that the vessel is a large source of gas. Outgassing rate also drops only slightly during the experiment. The outgassing experiment also included an analysis of the gas. This is mainly water vapor (90%) and nitrogen (10%).

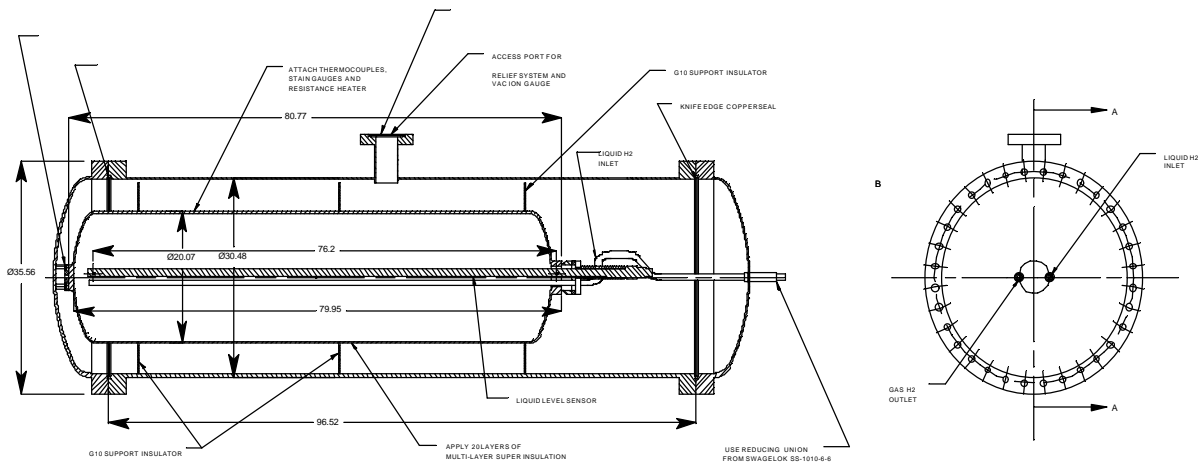


**Figure 9. Insulation design for pressure vessel. The figure shows a vacuum space, for obtaining high thermal performance from the multilayer insulation, and instrumentation for pressure, temperature and level. Dimensions are given in cm.**

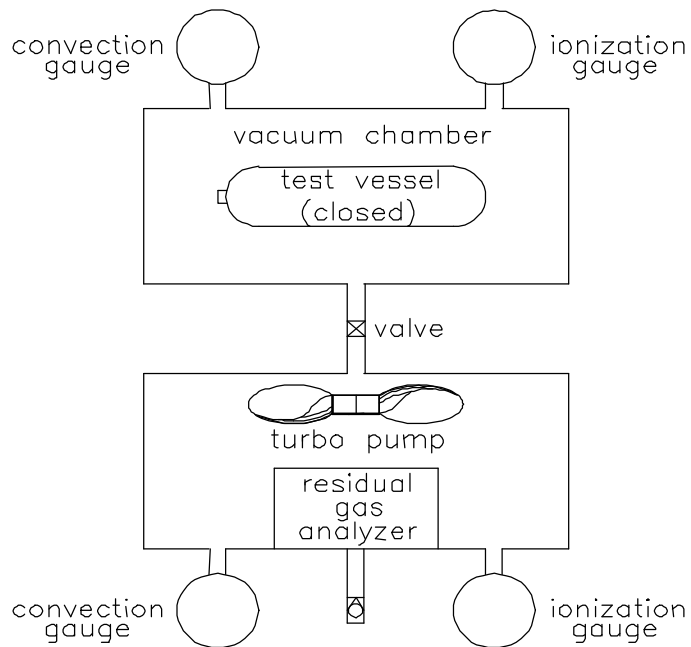


**Figure 10. Schematic of the experimental setup to investigate the outgassing rate of the pressure vessel material (fiber and epoxy) under vacuum conditions.**

Information on outgassing rates and composition will be used to calculate the type and quantity of adsorbent (getter) material necessary to keep the high vacuum required. A preliminary literature review (Carretti, 1995; Manini, 1997) indicates that it may be possible to use commercially available adsorbents for this application.

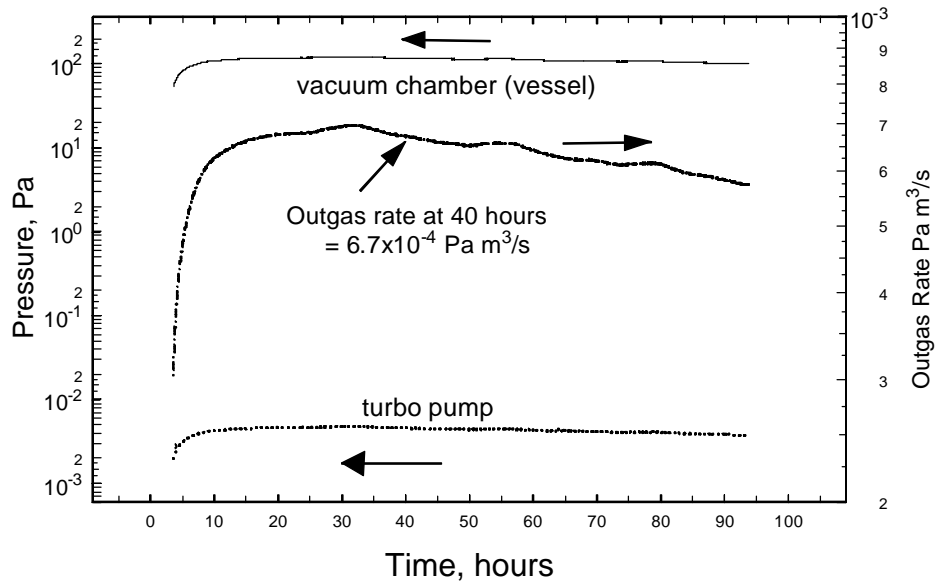


**Figure 11. Pressure of the turbo pump and vacuum chamber and outgassing rate as a function of time during the pressure vessel outgassing experiment.**

### **Pressure Test and Cryogenic Temperature Shock Conditioning**

The aramid-aluminum pressure vessel insulated with MLVSI will be pressure tested and shock-conditioned. Pressure and shock test will be done in preparation for liquid hydrogen fill tests, described in the next section. The vessel will be equipped with temperature, pressure and level sensors, necessary for determining the amount of fluid contained in the vessel. The experimental setup for this test is the same as previously used for cyclic testing (Figure 3). The test procedure will be as follows: The vessel will be pressurized with compressed helium to 1.2 times the Maximum Allowable Working Pressure (MAWP). The pressure will be held for a minimum of 30 minutes. Then, the pressure vessel will be shock conditioned by cycling it 3 times to low temperature with liquid nitrogen. Finally, The vessel will be leak tested with helium to 0.25 times the MAWP. Any leakage detected with a mass spectrometer leak detector is unacceptable.

## Testing of a Pressure Vessel with Liquid and Gaseous Hydrogen

The shock tested insulated pressure vessels will be transported to a remote facility for testing with liquid and gaseous hydrogen. Testing will involve filling the vessel with LH<sub>2</sub> to study the insulation performance, the accuracy of the sensors, and the problems involved with pumping the LH<sub>2</sub> into the vessel. The vessel will also be pressurized with compressed hydrogen to the working pressure. This test is expected to replicate what would happen to the vessel during fueling and operation in an LH<sub>2</sub>-fueled car.

### Future Work

Future plans include testing of insulated pressure vessels to a level equivalent to those used for pressure vessel certification by institutions such as the Department of Transportation (DOT), the Society of Automotive Engineers (SAE) and the National Fire Protection Association (NFPA). These institutions have established test procedures for pressure vessels that guarantee safety under regular operating conditions. A list of required tests has been extracted from the standards. Successful completion of these tests by insulated pressure vessels will guarantee a level of safety comparable to certification by DOT, SAE and NFPA. The list of planned tests is:

- Cycling, ambient temperature. 10000 cycles from less than 10% of the service pressure to the service pressure, 10 cycles per minute maximum (CFR-DOT, Title 49, 1996a). Each test cylinder must withstand the cycling pressurization test without any evidence of visually observable damage, distortion, or leakage.
- Cycling, environmental. 10 cycles per minute maximum. 1) 5000 cycles from zero to service pressure with tank at 60°C (140°F) and air at ambient temperature and 95% humidity, 2) 5000 cycles from zero to service pressure with tank at -51.1°C (-60°F) and air at ambient temperature, 3) 30 cycles from zero to service pressure, ambient conditions 4) burst test the cycled vessel (CFR-DOT, Title 49, 1996a). Each test cylinder must withstand the cycling pressurization test without any evidence of visually observable damage, distortion, or leakage.
- Cycling, Thermal. 10 cycles per minute maximum. 1) 10 000 cycles from zero to service pressure at ambient temperature, 2) 20 thermal cycles with tank temperature varying from 93.3°C (200°F) to -51.1°C (-60°F) at service pressure, 3) burst test the cycled vessel (CFR-DOT, Title 49, 1996a). Each test cylinder must withstand the cycling pressurization test without any evidence of visually observable damage, distortion, or leakage.
- Hydraulic Burst. Pressurize the cylinder to the required minimum burst pressure, and hold at that pressure for a minimum of 60 seconds. Increase the pressure to failure (CFR-DOT, Title 49, 1996a). In no case may the burst pressure of any cylinder be less than the required minimum burst pressure.
- Gunfire. Pressurize vessel with air or nitrogen to service pressure, and impact the vessel with a 0.30 caliber armor-piercing projectile with a speed of 853 m/s (2800 ft/s). The cylinder is positioned in such a way that the impact point is in the cylinder side wall at a 45° angle with

respect to the longitudinal axis of the cylinder. The distance from the firing location to the cylinder may not exceed 45.7 meters (150 feet) (CFR-DOT, Title 49, 1996a). The cylinder shall not fail by fragmentation.

- Bonfire. Pressurize cylinder with air or nitrogen to service pressure. Set pressure relief devices to discharge at 83% of the cylinder test pressure. The cylinder shall be exposed to fire until the gas is fully vented. The temperature measured in the surface tank exposed to the fire has to be between 850 and 900°C (CFR-DOT, Title 49, 1996a). The venting of the gas must be predominantly through the pressure relief device.
- Stress Analysis (yield strength, tensile strength, and elongation). Cut pieces from tank (aluminum and composite) and test in universal machine (CFR-DOT, Title 49, 1996a). Procedures and results have to be according to the ASTM standards.
- Drop Test from 3 m (10 ft). 1) The cylinder is dropped vertically onto the end, 2) the cylinder is dropped horizontally onto the side wall, 3) the cylinder is dropped onto a 3.8 x 0.48 cm (1 ½ x 3/16 inch) piece of angle iron, 4) after the drops, the vessel is cycled over 1000 pressure cycles from 10% of service pressure to the service pressure, at 10 cycles per minute (CFR, Title 49, 1996). The cylinder then has to be burst tested; the burst pressure of this vessel has to be at least 90 % of the minimum burst pressure.
- Drop tests from 10 m and 3 m. 1) Drop from 10 m. The drop test subjects a full-size vehicle fuel tank to a free-fall impact onto an unyielding surface from a height of 10 m. The fuel tank is released by firing one or more explosive cable cutters simultaneously. The fuel tank impacts the outer shell on the critical area as determined by the manufacturer. The fuel tank is filled with an equivalent full weight of liquid nitrogen saturated to at least 1/2 the maximum allowable working pressure of the fuel tank. 2) Drop from 3 m. The drop test subjects a full-size vehicle fuel tank to a free-fall impact onto an unyielding surface from a height of 3 m. The fuel tank is released by firing one or more explosive cable cutters simultaneously. The fuel tank impacts the outer shell on the critical area as determined by the manufacturer. The fuel tank is filled with an equivalent full weight of liquid nitrogen saturated to at least 1/2 the maximum allowable working pressure of the fuel tank (SAEJ2343, 1997). There shall be no loss of product for a period of 1 hour after the drop other than relief valve operation and loss vapor between the filler neck and the secondary relief valve in the case of a test involving the filler neck. Loss of vacuum, denting of the vessel, piping and piping protection, and damage to the support system are acceptable.
- Flame test. The tank should contain an equivalent full level of liquid nitrogen saturated at one half the maximum allowable working pressure (MAWP). The tank should be inverted and subjected to an external temperature of 538°C (1000°F) for 20 minutes without the vessel reaching relief pressure (SAE J2343, 1997)
- Test of welds (tensile, guided bend, alternate guided-bend, impact) (CFR-DOT, Title 49, 1996b; NFPA 52, 1998).

- Radiographic examination. One finished longitudinal seam shall be selected at random from each lot and radiographed throughout its entire length (CFR-DOT, Title 49, 1996a).

Future plans include the installation of insulated pressure vessels into demonstration hydrogen-powered vehicles. For this application, the NFPA (NFPA 57, 1996; NFPA 52, 1998), and CFR-DOT (Title 49, 1996a) standards will be reviewed to prepare the required tests to guarantee the safety of the operation.

### **Acknowledgments**

This project is funded by the DOE Hydrogen Program, Sig Gronich and Neil Rossmesl, Program Managers. The authors also express their appreciation for the significant contributions of Structural Composites Industries (SCI) to this project. Work performed under the auspices of the U.S. Department of Energy by Lawrence Livermore National Laboratory under Contract W-7405-ENG-48.

### **References**

Aceves, S. M., Berry, G.D., 1998, "Thermodynamics of Insulated Pressure Vessels for Vehicular Hydrogen Storage," ASME Journal of Energy Resources Technology, June, Vol. 120, pp. 137-142.

Bray, D.E., and Stanley, R.K. 1997, "Nondestructive Evaluation: A tool in Design, Manufacturing, and Service," CRC Press, Boca Raton, FL.

Braess, H.H., and Strobl, W., 1996, "Hydrogen as a Fuel for Road Transport of the Future: Possibilities and Prerequisites," Proceedings of the 11<sup>th</sup> World Hydrogen Energy Conference, Stuttgart, Germany.

Code of Federal Regulations, Department of Transportation (CFR-DOT), 1996a, "Basic Requirements for Fully Wrapped Fiber Reinforced Aluminum Lined Cylinders," Title 49, CFR 107.105 Standard.

Code of Federal Regulations, Department of Transportation (CFR-DOT), 1996b, "Welded Cylinders Insulated," Title 49, 178.57 Specification 4L.

Corretti, C. 1995, "General Introduction to Outgassing Data and Measurement Methods," Gas-Surface Laboratory, SAES Getters S.p.A, Viale, Italy.

Hettinger, W. Michel, F., Ott, P., and Theissen, F., 1996, "Refueling Equipment for Liquid Hydrogen Vehicles," Proceedings of the 11<sup>th</sup> World Hydrogen Energy Conference, Stuttgart, Germany, pp. 1135-1143.

Hull, D., and Clyne, T.W., 1996, "An Introduction to Composite Materials," Cambridge University Press, Cambridge, Great Britain.



Institute of Gas Technology, 1996, "Compressed Natural Gas Storage Optimization for Natural Gas Vehicles," Gas Research Institute Report GRI-96/0364, Des Plaines, IL.

Kaganer, M.G., 1969, "Thermal Insulation in Cryogenic Engineering," Israel Program for Scientific Translation Ltd., Jerusalem, Israel.

Manini, P. 1997, "The Combogetter™ as a Key Component in the Vacuum Insulated Panels (VIPs) Technology," *Vuoto*, Vol. 26, No. 2, pp.45-53.

Michel, F., Fieseler, H., Meyer, G., and Theissen, F., 1996, "Onboard Equipment for Liquid Hydrogen Vehicles," Proceedings of the 11<sup>th</sup> World Hydrogen Energy Conference, Stuttgart, Germany, pp. 1063-1077.

Morgan, R.J. and Allred, R.E., 1989, "Aramid fiber reinforcements," in "Reference Book for Composite Technology," Edited by Lee, S.M., pp. 143-166, Technomic Publishing, Lancaster, PA.

National Fire Protection Association (NFPA), 1998, "NFPA 52: Compressed Natural Gas (CNG) Vehicular Fuel System Code," Quincy, MA.

National Fire Protection Association (NFPA), 1996, "NFPA 57: Liquefied Natural Gas (LNG) Vehicular Fuel System Code," Quincy, MA.

Pehr, K., 1996a, "Experimental Examinations on the Worst Case Behavior of LH<sub>2</sub>/LNG Tanks for Passenger Cars," Proceedings of the 11<sup>th</sup> World Hydrogen Energy Conference, Stuttgart, Germany.

Pehr, K., 1996b, "Aspects of Safety and Acceptance of LH<sub>2</sub> Tank Systems in Passenger Cars," *International Journal of Hydrogen Energy*, Vol. 21, pp. 387-395.

Pentastar Electronics, 1997, "Direct-Hydrogen-Fueled Proton-Exchange-Membrane Fuel Cell System for Transportation Applications, Conceptual Design Report," Report DOE/CE/50390-9, prepared for U.S. Department of Energy, Office of Transportation Technologies, under contract DE-AC02-94CE50390.

Peschka, W., 1992, "Liquid Hydrogen, Fuel of the Future," Springer-Verlag, Vienna, Austria.

Reed, R.P., and Golda, M., 1994, "Cryogenic Properties of Unidirectional Composites," *Cryogenics*, Vol. 34, No. 11, pp. 909-928.

Society of Automotive Engineers (SAE), 1997, "Recommended Practices for LNG Powered Heavy-Duty Trucks," SAE.J2343.

Wetzel, F.J., 1996, "Handling of Liquid Hydrogen at Filling Stations," Proceedings of the 11<sup>th</sup> World Hydrogen Energy Conference, Stuttgart, Germany, pp. 1123-1134.